Monthly Bulletin

Institut de physique du globe de Paris
Observatoire volcanologique du Piton de la Fournaise

ISSN 2610 – 5101

March, 2026

PITON DE LA FOURNAISE *(VNUM #233020)*
Latitude: *21.244°S*
Longitude: *55.708°E*
Summit elevation: *2632 m*

Piton de la Fournaise is a basaltic hot spot volcano located in the southeastern part of La Réunion Island (Indian Ocean). The volcano first erupted about 500,000 years ago. Its volcanic activity is characterized by frequent effusive eruptions (with emissions of lava fountains and lava flows) that occur on average twice a year since 1998. More rarely, larger explosive eruptions (with blocks covering the summit area and ash emissions that can disperse over long distances) have happened in the past with a centennial recurrence rate.
Most of the current eruptive activity (97% during the last 300 years) occurs from vents inside the Enclos Fouqué caldera. A few eruptions, however, have occurred from vents outside the caldera (most recently in 1977, 1986, and 1998). Such eruptions can potentially threaten communities that live in the surrounding areas.
Since late 1979, the activity of Piton de la Fournaise is monitored by the Piton de la Fournaise Volcanological Observatory (Observatoire Volcanologique du Piton de la Fournaise - OVPF), which belongs to the Institut de Physique du Globe de Paris (IPGP).

Alert level: Alert 2-2
(from March, 12 2026)

February 13 to March 12 (10h) 2026: Alert 2-1 ***(cf. table in the appendix)***

Institut de physique du globe
de Paris, OVPF
14 RN3 – Km 27
97418 La Plaine des Cafres
La Réunion

www.ipgp.fr/ovpf
facebook : ObsVolcanoPitonFournaise
bluesky : @ovpf.bsky.social
youtube : Chaîne IPGP

A. Piton de la Fournaise activity

Seismicity

The seismological network of the Piton de la Fournaise Volcanological Observatory consists of 41 seismological stations currently in operation, representing a total of 109 channels sampled at 100 Hz and transmitted in real time to the observatory. This network includes 32 three-component broadband stations, 2 three-component short-period stations and 7 analogue stations with one vertical component. ***Due to the eruption that started on Februry 13, 2026, two seismic stations (the PVD and GPS stations) threatened by lava flows had to be urgently dismantled by OVPF teams, with assistance from Section Aérienne de Gendarmerie and Peloton de Gendarmerie de Haute Montagne.***
Earthquakes are located based on the arrival times of P and S waves, which are manually plotted in the SeisComP software (www.seiscomp.de) using automatic or visual detections. The earthquakes are then located using NonLinLoc software (Lomax et al., 2000), using a three-dimensional velocity model. This model takes into account a velocity gradient according to the topography and assumes a constant VP/VS ratio of 1.7. The P-wave velocity is 3.3 km/s at the free surface and increases linearly with depth at a gradient of 0.3 s^{-1}.

Observations

In March 2026, the OVPF-IPGP recorded at Piton de La Fournaise:

- 901 shallow volcano-tectonic earthquakes (0 to 2.5 km above sea level) below the *Bory* and *Dolomieu* summit craters;
- 17 deep volcano-tectonic earthquakes (below sea level);
- 40 long-period earthquakes;
- 146 rockfalls;
- as well as the recording of a tremor associated with the eruption that started on February 13, 2026, and continued into March 2026 (see section B for more details).

The amplitude of the tremor (an indicator of lava and gas emission at the surface) increased sharply at the start of the eruption before dropping, as is typically observed during the first few hours of an eruption at Piton de la Fournaise (Figure 1).
. In early March, the tremor showed a gradual increase until March 11, when a sudden drop in amplitude was recorded. This decrease was associated with a slowdown of the lava flow front on the steep slopes (see OVPF release of March 12, 2026). It may potentially be related with the reopening of the eruptive cone, which had been progressively closing since late February. However, poor visibility prevents confirmation of this interpretation.
. Subsequently, the eruptive tremor increased until March 18, followed by a decrease and the observation of numerous **"gas piston" sequences or tremor bursts**. These tremor bursts show a clear correlation with activity at the eruption site, marked by alternating phases of calm associated with weak tremor and phases of lava fountains with active degassing and significant tremor levels (Figure 2).
. **On March 25, several sharp drops in eruptive tremor were observed** between 5:50 a.m. UTC and 9:45 a.m. UTC**, prior to the cessation of surface eruptive activity.** A very weak residual tremor subsequently appeared on the spectrograms from the FOR station (located near the eruption site), although no lava or gas emissions were observed at the eruption site.
. **Eruptive activity resumed on March 28** with a very gradual increase in tremor beginning at 9:00 UTC, then accelerating after 15:00 UTC. Through the end of March, the tremor remained relatively stable, at a level comparable to that observed before the cessation of surface eruptive activity on March 25.
. At the time of writing this bulletin, **the eruption had stopped again during the night of April 2–3 around 12:10 a.m. local time (8:10 p.m. UTC on April 2)**.

Regarding seismic activity beneath Piton de la Fournaise in March 2026, a resumption and **increase in summit volcano-tectonic earthquakes began on March 18, coinciding with the deflation of the edifice** (see next section) until the eruption stopped on March 25 (Figure 3). When the **eruption stopped, deep seismicity was observed between 6 and 8 km below sea level** (Figures 3 and 4)**, accompanied by long-period earthquakes** (Figure 3). Since the resumption of the eruption on March 28, and in the

same time as a deflation of the volcanic edifice was again recorded, a new increase in summit volcano-tectonic seismicity has been observed (Figure 3).

In addition, **146 rockfalls** were detected during the month, mainly inside the *Dolomieu* crater, along the cliffs of the *Enclos Fouqué* caldera and of the *Cassé de la Rivière de l'Es*t, and on the recently formed cone and lava flows. This type of gravitational activity is common at Piton de la Fournaise

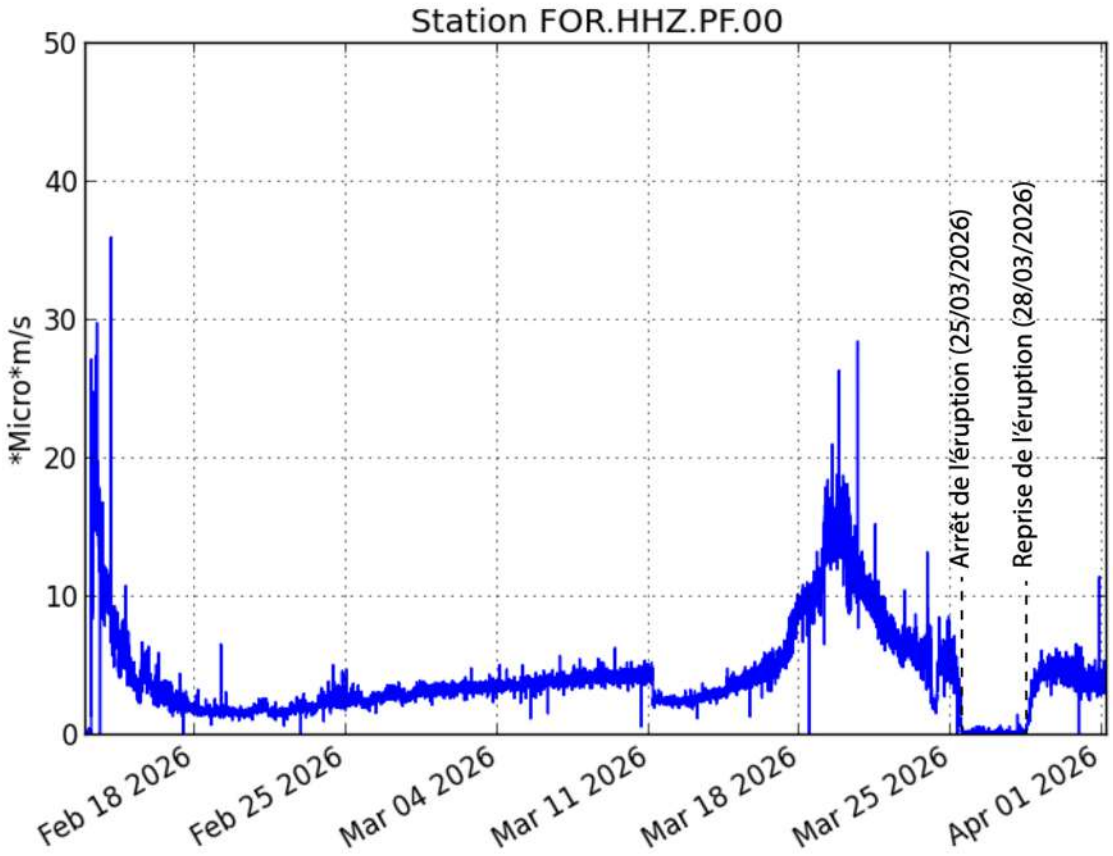

Figure 1: Evolution of the eruptive tremor amplitude between February 13 and April 1st 2026 (©WebObs/OVPF-IPGP).

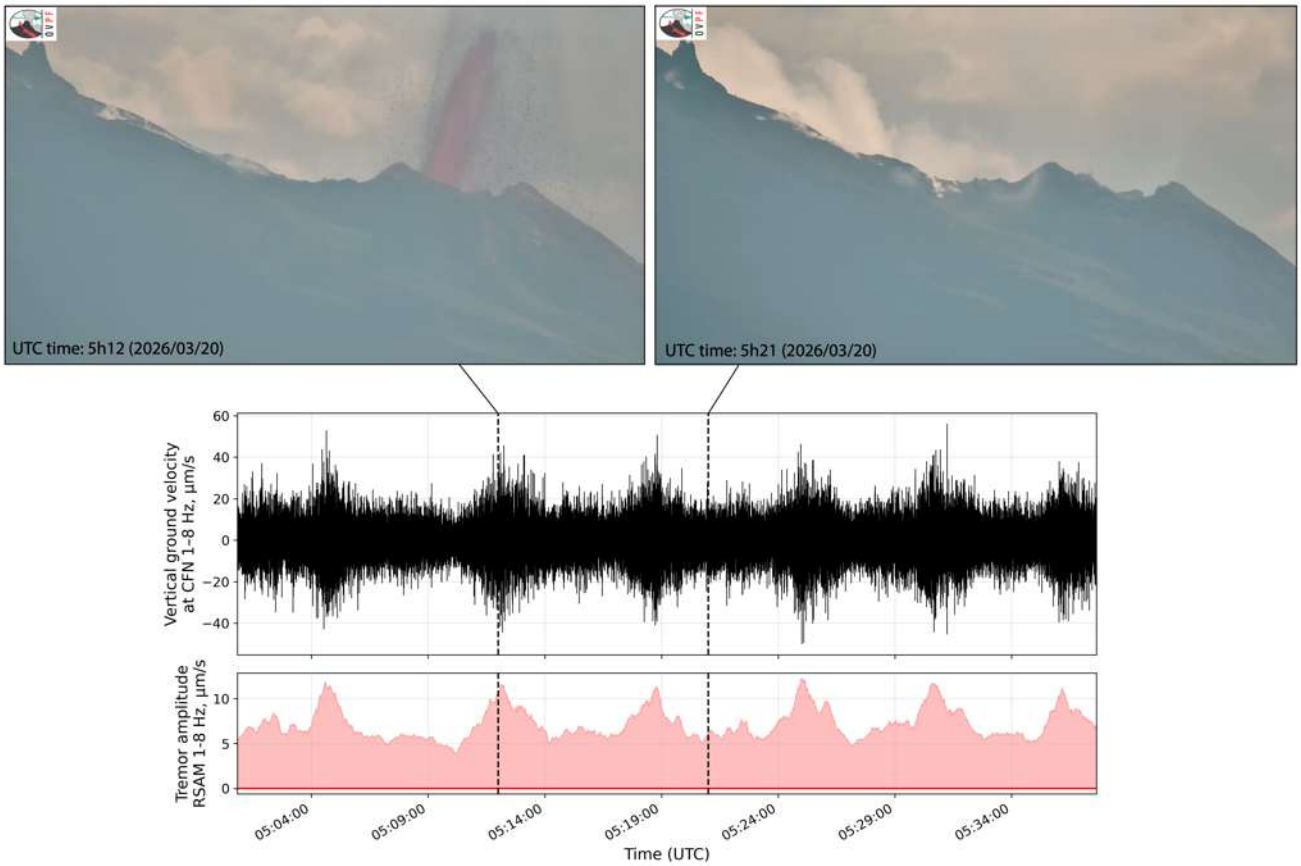

Figure 2: Comparison of the amplitude of the tremor recorded at the CFN station (bottom) and surface lava fountain activity (top) on March 20, 2026, between 5:00 and 5:40 UTC. The "piston gas" or tremor bursts are clearly linked here to intermittent degassing associated with phases of lava fountain activity (at 5:12 UTC, top left) and quiet phases with few visible projections (at 5:21 UTC, top right) (©OVPF-IPGP).

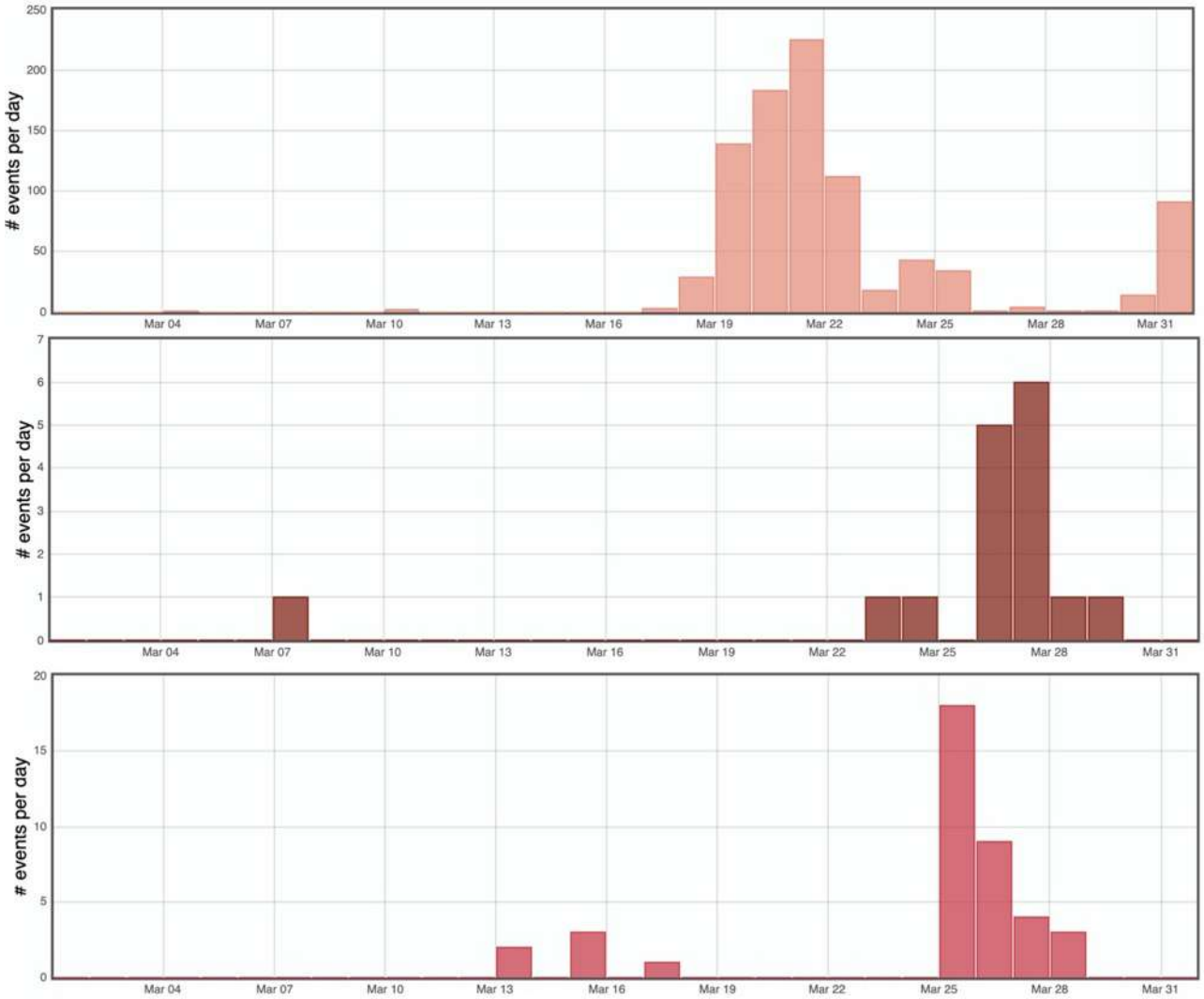

Figure 3: Number of (top) shallow volcano-tectonic, deep volcano-tectonic (middle) and long-period (bottom) earthquakes per day recorded in March 2026 (©WebObs/OVPF-IPGP).

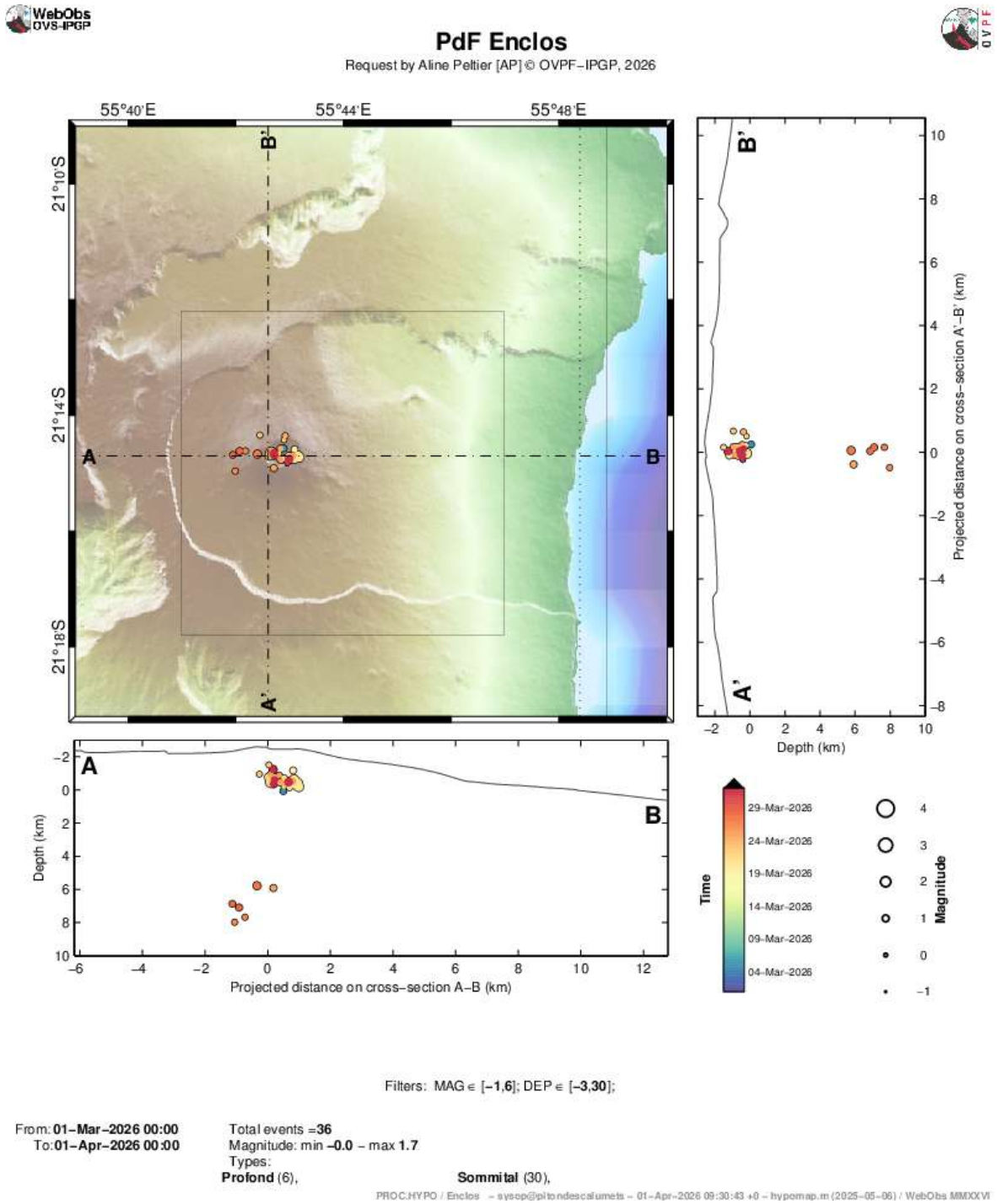

Figure 4: Seismicity below Piton de la Fournaise in March 2026. Location map (epicenters) and north-south and east-west cross-sections (hypocenters) of earthquakes as recorded by OVPF-IPGP. Only manually located earthquakes are shown on the map (©WebObs/OVPF-IPGP).

Deformation

The permanent network for monitoring deformation at Piton de la Fournaise currently comprises:
- 27 GNSS (Global Navigation Satellite System) stations,
- 11 pairs of tiltmeters at 10 different sites,
- 3 three-component extensometers.
Once the data have been retrieved (every 15 min to every day depending on the stations), they are automatically processed using the GipsyX/JPL software (Bertiger et al., 2020; Murphy et al., 2024).
These calculations incorporate the new JPL products in ITRF2020 (Altamimi et al., 2023, Rebischung et al., 2024). The calculated coordinates are expressed relative to the Figure Centre (FC), a concept more suited to small-scale area of work.

Observations

Following the dike opening on February 13, 2026, which generated displacements of about 30 cm along the southern outer rim of the *Dolomieu* crater and about 40 cm along the south-east flank (see the February 2026 monthly bulletin from the OVPF-IPGP), a slight deflation of the edifice was recorded until around February 22, linked to the transfer of magma from the magma feeding system located beneath the summit toward the eruptive site (Figures 5 and 6).

Between February 24 and March 15, inflation of the summit area was recorded, indicating repressurization of the volcano's feeding system located beneath the summit area (Figures 5, 6, and 7). This inflation is believed to be linked to the ascent of magma from depth toward the shallow magma reservoir, subsequently contributing to feeding the eruption.

Between March 16 and March 23, 2026, **deflation of the whole edifice was recorded**, with a sharp decrease in the baseline crossing the summit (Figures 5, 6 and 7), before inflation resumed and continued until the resumption of activity on March 28.
The resumption of inflation at the summit stations occurred later and was recorded during the stop of the eruption from March 25 to 28, 2026 (Figures 5, 6 and 7).

Numerical modelling

Modelling of the deformation sources for the two main periods of inflation (February 24–March 15) and deflation (March 16–March 23) shows the activation of a common source located 1.3–1.6 km above sea level (1 km below the surface of the Dolomieu crater, Figure 8), corresponding to the position of the shallow magma reservoir located at a depth of 1.5–2 km and most certainly including a component of the dike* feeding the eruption.

1. From February 24 to March 15, 2026, the influence of a second, deeper source in deflation at 15 km below sea level was superimposed on this shallow source, which was then in inflation (Figure 8, left);
2. From March 16 to 23, 2026, the influence of a second, deflating source located 2 km below sea level was superimposed on this shallow source, which was then in deflation (Figure 8, right).

** Dike: an intrusion of magmatic rock; in this case located between the shallow reservoir and the surface, which feeds the eruption. It is a planar structure, generally 1–2 m thick and capable of propagating over hundreds of meters or even several kilometers.*

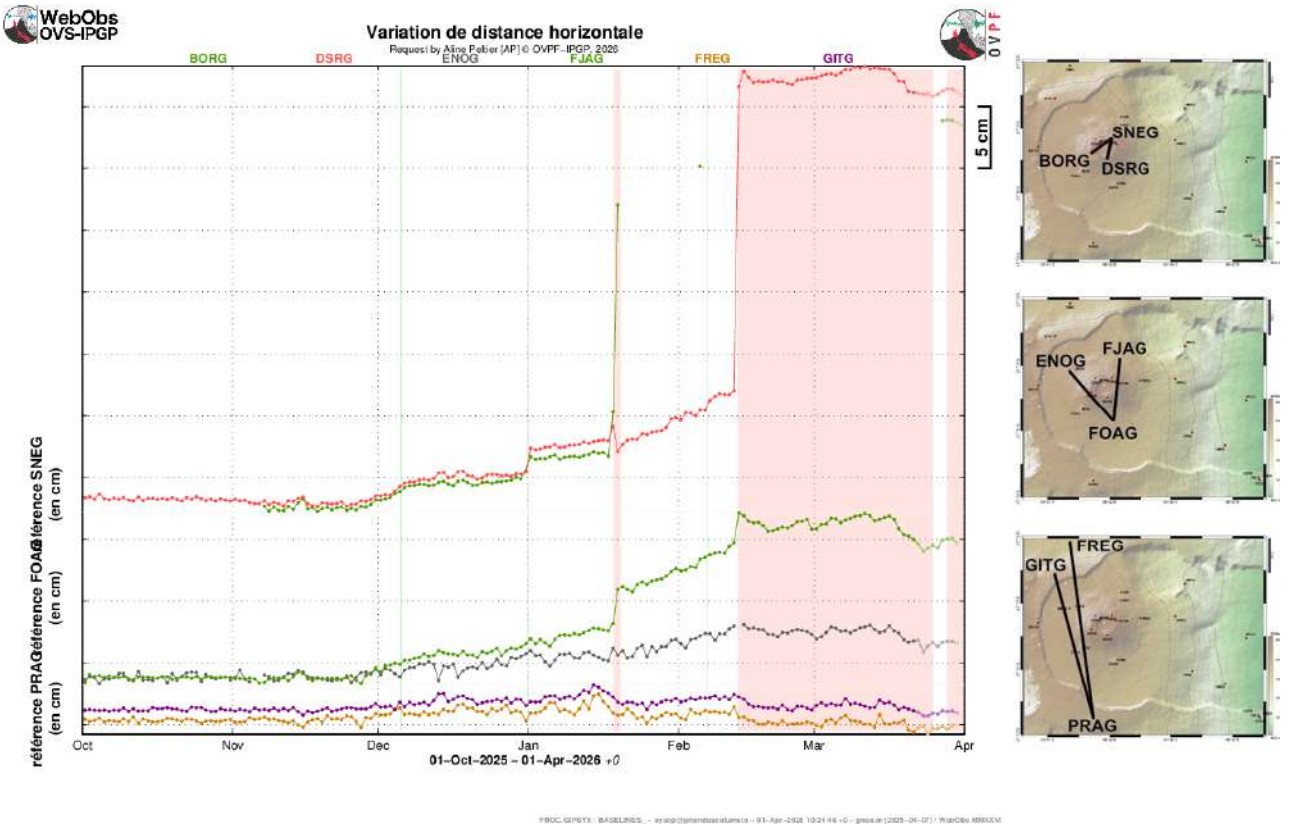

Figure 5: Ground deformation records over the past six months (the red and green bars represent eruptive and intrusive periods, respectively). The time series plots show the changes in horizontal distance between pairs of GNSS stations located around the Dolomieu summit crater (reference: SNEG; top graph), the terminal cone (reference: FOAG; middle graph) and the Enclos Fouqué caldera (reference: PRAG; bottom graph), from north to south (see location on the right). Increasing distances (or baseline elongation) indicate volcano inflation, while decreasing distances (or baseline contraction) reflect edifice deflation (©Webobs/OVPF-IPGP).

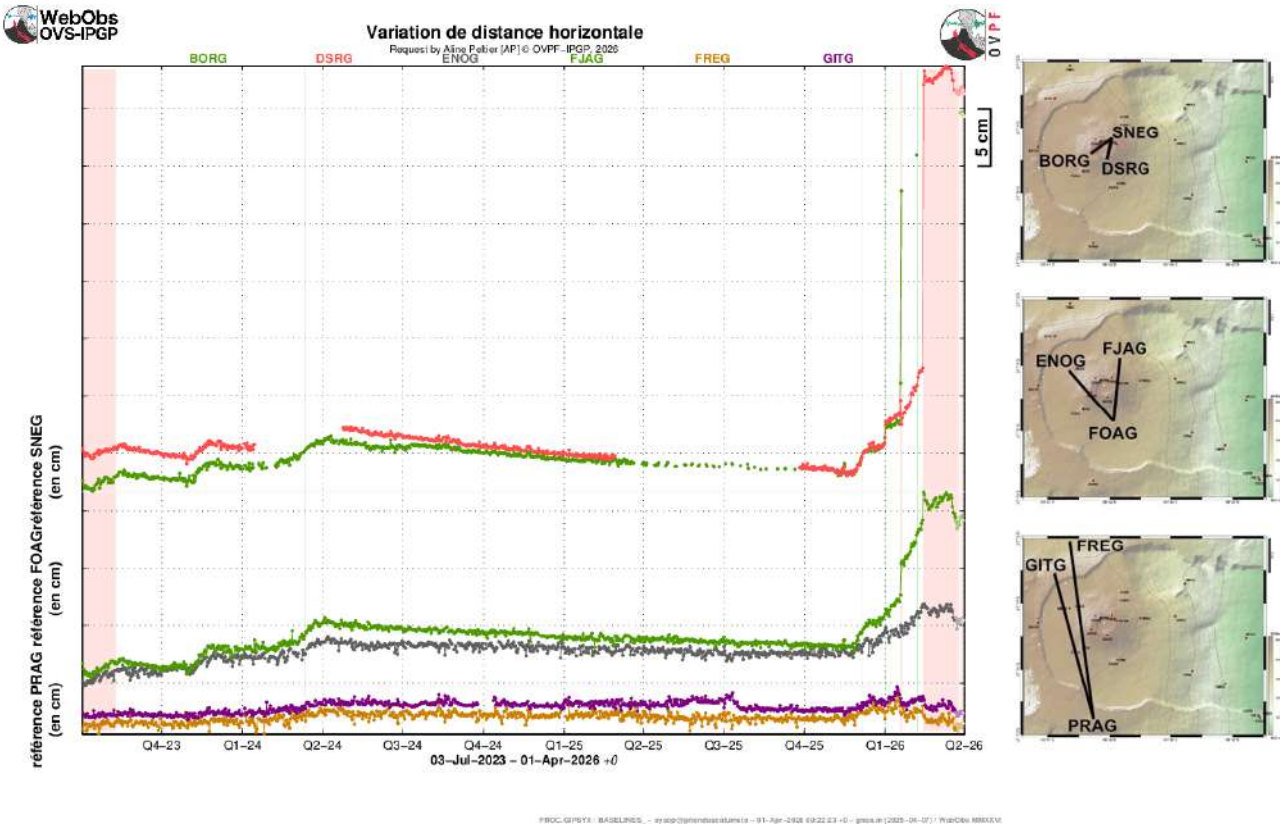

Figure 6: Ground deformation records since the eruption of July-August 2023 (the red and green bars represent eruptive and intrusive periods, respectively). The time series plots show the changes in horizontal distance between pairs of GNSS stations located around the Dolomieu summit crater (reference: SNEG; top graph), the terminal cone (reference: FOAG; middle graph) and the Enclos Fouqué caldera (reference: PRAG; bottom graph), from north to south (see location on the right). Increasing distances (or baseline elongation) indicate volcano inflation, while decreasing distances (or baseline contraction) reflect edifice deflation (©WebObs/OVPF-IPGP).

** Glossary: The summit GNSS signals indicate the influence of a shallow pressure source below the volcano, while distant GNSS signals indicate the influence of a deep pressure source below the volcano. Inflation usually means pressurization; and conversely deflation usually means depressurization.*

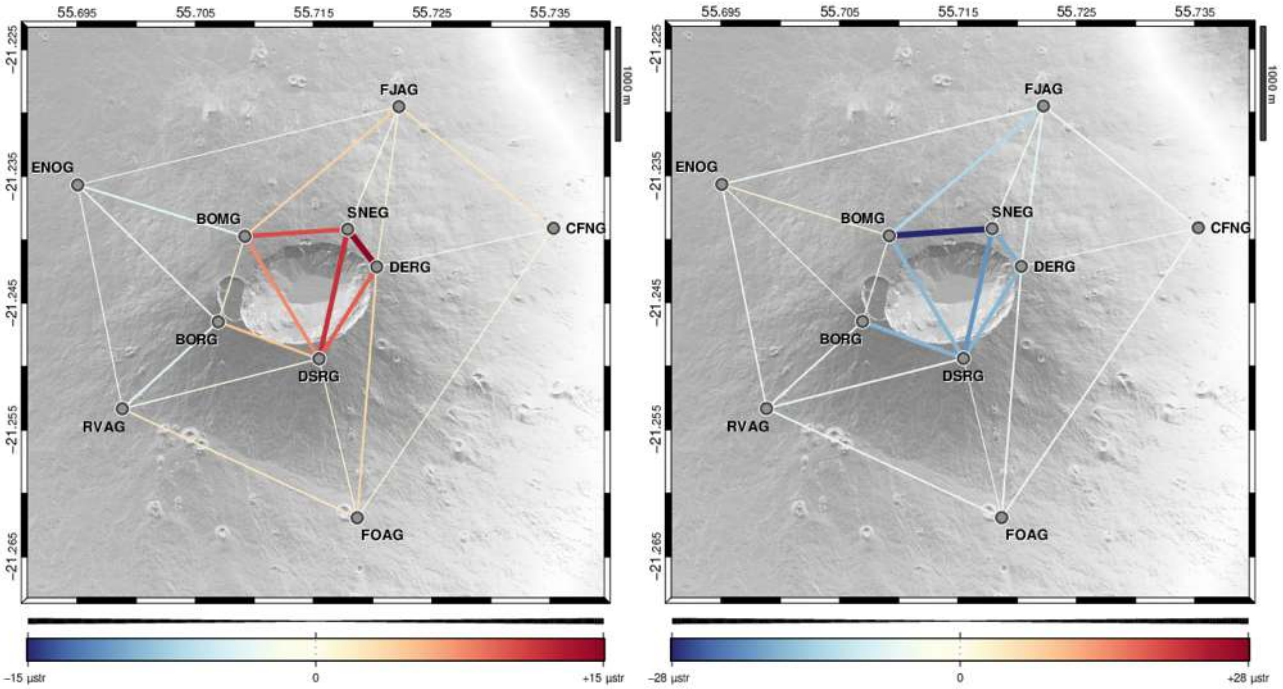

Figure 7: Linear 3-D strain maps (in microstrain) for (left) the inflation period from February 24 to March 15, 2026, and (right) the deflation period from March 16 to March 23, 2026. The thickness and color of the baselines indicate the intensity of the strain, either compressive (in blue) or tensile (in red) (©WebObs/OVPF-IPGP, topography ©IGN LIDAR 2025).

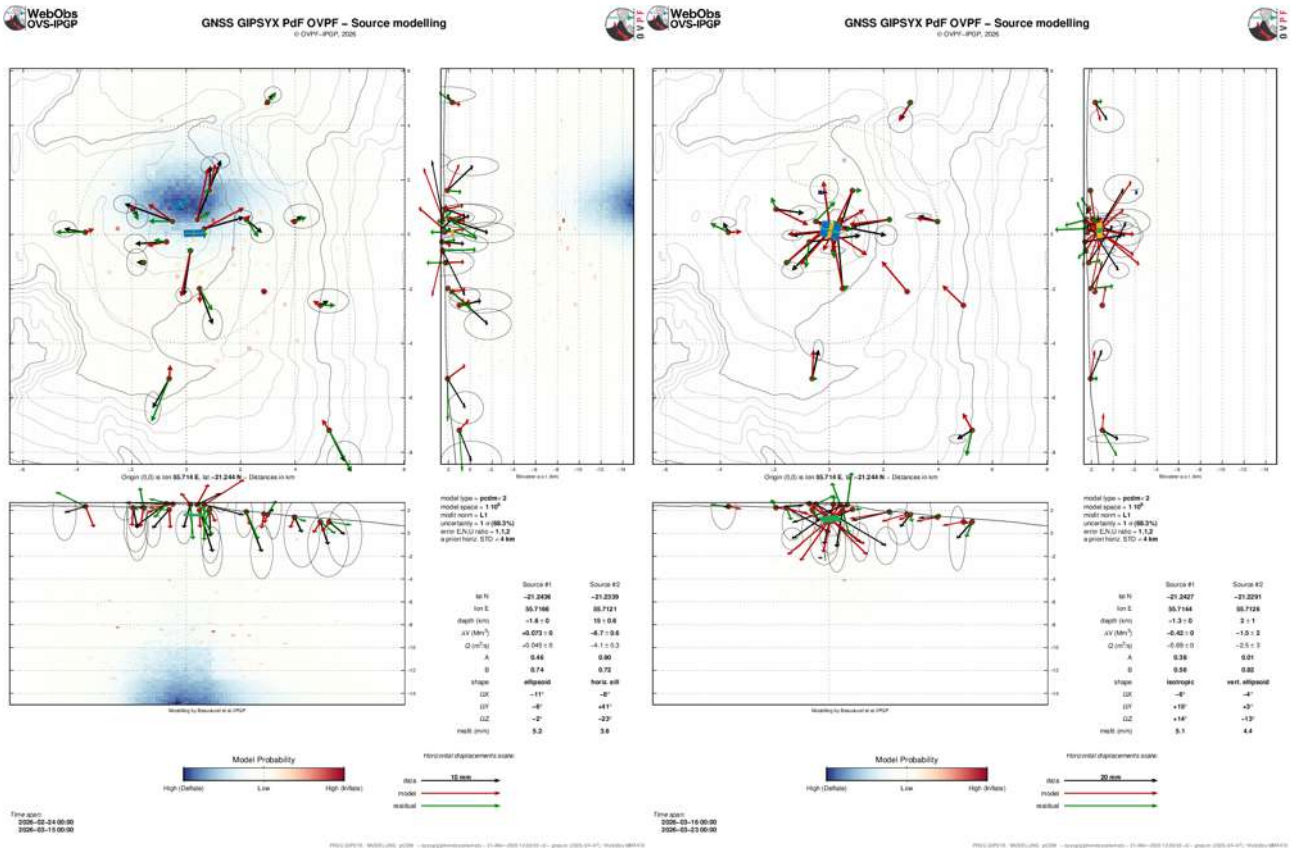

Figure 8: Modelling of the pressure sources responsible of ground displacements (pCDM models) linked (left) to the inflation period of February 24 to March 15 and (right) to the deflation period of March 16 to 23. The black vectors represent observed data, the red vectors represent modelled vectors, and the green vectors represent the residuals between observed and modelled vectors. The characteristics of each source (primary #1 and secondary #2) are listed in the lower right corner (©Webobs/OVPF-IPGP).

Gas geochemistry

The permanent geochemical network for monitoring gas emissions from Piton de la Fournaise currently comprises:
- 3 MAX-DOAS stations measuring the optical thickness of SO2 (ppm.m) in the atmosphere. Measurements are taken every 10 to 15 minutes during the day when weather conditions are favorable (Arellano et al., 2020).
- 1 MultiGaS station measuring excess H2O, CO2, SO2 and H2S relative to the atmosphere, with measurements taken every 6 hours.
- 4 stations measuring CO2 flux through the soil. At these stations, meteorological parameters (temperature, pressure, humidity, wind speed and direction) are also recorded in order to correct signals from environmental disturbances (Boudoire, 2017; Bénard et al., 2023). Measurements are taken every hour.

Due to a technical issue, the graphs showing CO_2 concentrations in the soil and the data from the MultiGas station at the summit of the volcano cannot be shown this month.

SO_2 flux in the air obtained by DOAS method

The NOVAC stations located on the edges of the Enclos Fouqué (“Enclos0” to the west, “Piton de Bert” to the south, and “Piton Partage” to the north) detected the gas plume associated with the eruption that start on February 13, 2026.

The start of the February 2026 eruption was associated with a very high SO_2 flux (up to 10 kton/day on February 13). These emissions decreased rapidly between February 13 and 15. These SO_2 fluxes are shown in section B of this bulletin (Figure 16).

** Glossary: During rest periods, SO_2 flux at Piton de la Fournaise is below the detection threshold. The SO_2 flux may increase during magma transfer in the shallowest part of the feeding system. During eruptions, it is directly proportional to the amount of lava emitted at the surface.*

Phenomenology

March 2026 was marked by the **continuation of the eruption that started on February 13, 2026, with a stop in the surface activity observed between March 25 (4:30 p.m. local time) and March 28 (3:00 p.m. local time)** (see section B for more details). At the time of writing this bulletin, **the eruption had stopped again during the night of April 2–3 around 12:10 a.m. local time (8:10 p.m. UTC on April 2)**. The end of this eruption will be discussed in the next monthly bulletin.

Summary

The eruption that started on February 13, 2026, continued throughout March 2026. A detailed summary is provided below in section B of this bulletin. The onset of the eruption and related observations were described in the February 2026 monthly bulletin.

B. The February 13, 2026 eruption

** Information regarding the onset of this eruption and its precursors can be found in the OVPF-IPGP monthly bulletin for February 2026.*

** Detailed day-by-day information can be found in the OVPF-IPGP's special daily bulletins, available at this link: https://www.ipgp.fr/communiques-et-bulletins-de-lobservatoire/?categorie=&domaine=&date=&observatoire-associe=391&motcle=*

Surface activity

Following the opening of four eruptive fissures on February 13 along the eastern and southeastern outer edges of the *Dolomieu* crater and on the volcano's east-southeastern flank, activity has been concentrated at a single eruptive site since February 14. This site is located on the lowest fissure, which opened on the east-southeast flank at an elevation of 2,056 meters.

The concentration of activity at a single site allowed for the formation of an eruptive cone created by the accumulation of lava projections and overflows (Figure 9), and the lava flows have gradually advanced toward the eastern flank of the volcano, with the development of lava tubes (flows confined beneath a solidified crust) that has allowed the lava to be isolated from the atmosphere and to resurface further downstream at numerous breakouts (Figure 10).

Figure 9: Photo of the eruptive cone taken on March 31, 2026, at 7:21 a.m. (©OSUL- Lyon 1 Université).

Figure 10: Photos of the lava field (lava tubes and lava flows) on March 10, 2026 (©OVPF-IPGP).

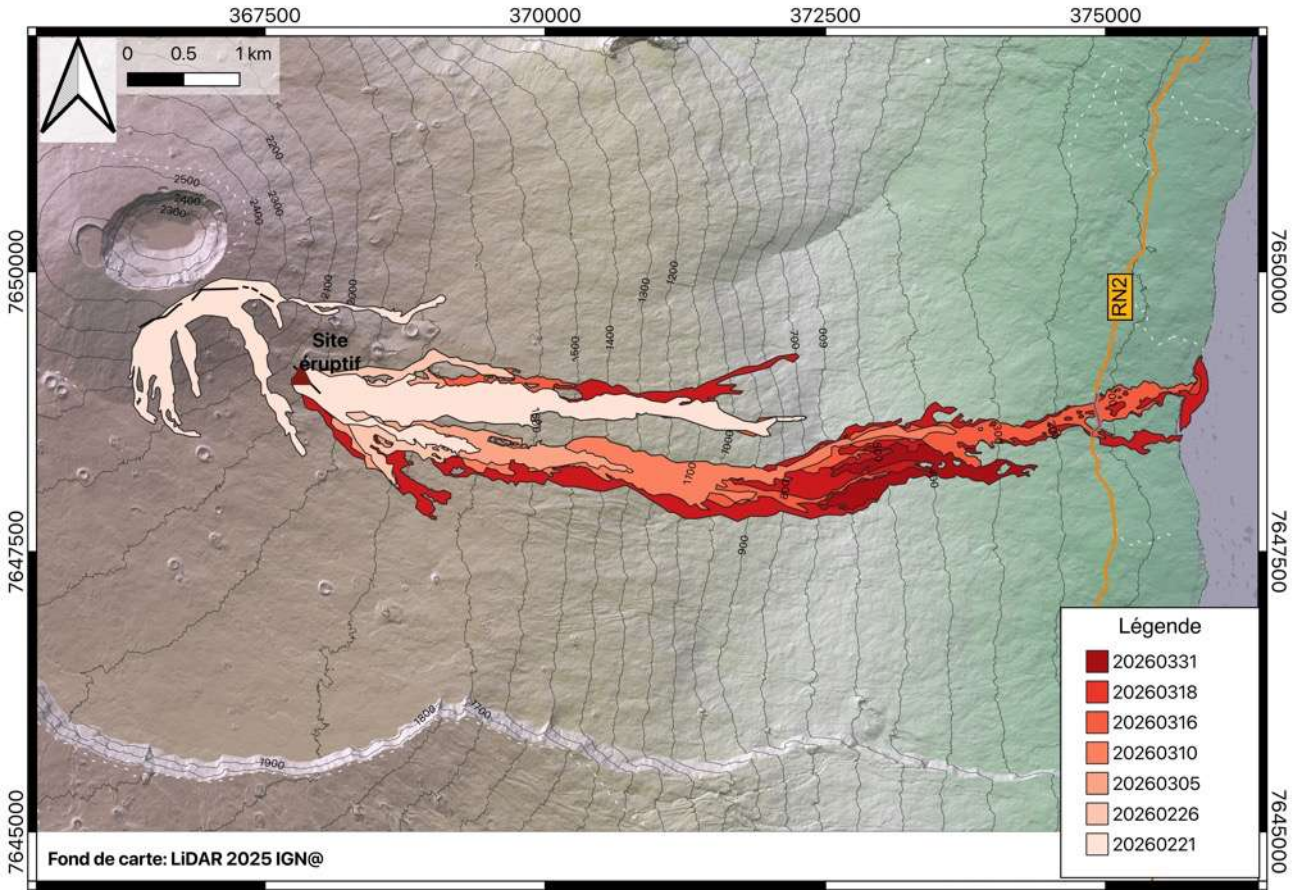

Figure 11: Map of lava flows associated with the eruption that started on February 13, 2026, at Piton de la Fournaise, as of March 31, 2026 (© OI²/ISDeform – OSUL, OPGP-LMV, Université de La Réunion, OVPF-IPGP).

The lava field that formed downstream of the eruptive cone has developed two main branches (north and south, Figure 11).

On March 12 at 10:00 a.m., **as the southern branch's flow front advanced—at that time located approximately 400 meters upslope from the road and posing a direct threat to it**—the prefecture raised the alert level of the ORSEC plan "*Volcan du Piton de la Fournaise*" to **Alert level 2-2** (see Appendix D for more details on this alert level).

Thus, one month after the eruption started, **on March 13 at 8:02 a.m. (local time), the southern branch's lava flow reached National Route 2**, located more than 7 kilometers from the eruptive site (Figure 12). Three days later, in the early hours of March 16 around 12:20 a.m., it finally reached the ocean, having traveled approximately 825 meters below the road (Figure 13).

At the point where the lava met the ocean, a platform formed as a result of the accumulation of lava flows and fine particles from the fragmentation of the lava, as well as a plume of acidic gas, called "laze" (lava haze), consisting of water vapor, hydrochloric acid (HCl), and fine particles (Figure 13).

Figure 12: Photos of lava flowing across Route 2 on March 13, 2026 (©OVPF-IPGP).

Figure 13: Photos of the platform (top) taken on March 16 (©OVPF-IPGP) and (bottom) on March 20 (©University of Réunion).

Institut de physique du globe
de Paris, OVPF
14 RN3 – Km 27
97418 La Plaine des Cafres
La Réunion

www.ipgp.fr/ovpf
facebook : ObsVolcanoPitonFournaise
bluesky : @ovpf.bsky.social
youtube : Chaîne IPGP

Lava flow rates

Lava flow rates, estimated from satellite data using the HOTVOLC (OPGC – Clermont Auvergne University) and MIROVA (University of Turin) platforms, reached values as high as 63 m³/s during the first hours of the eruption, then declined as activity on the first fissures ceased (Figure 14). Between February 16 and March 18, average lava flow rates were < 20 m³/sec and, most of the time, ranged between 1 and 10 m³/sec (Figure 14).

An increase in flow rates was recorded between March 17–18 and March 20 (peaking at 25 m³/sec). This increase occurred during the most intense deflation phase in the summit area (a deflation phase that lasted until March 23, Figure 15) and during the increase in shallow volcano-tectonic seismicity (located beneath the summit, Figure 4) that lasted from March 18 to 22 (Figure 15). This deflation phase, accompanied by increased shallow seismicity and higher flow rates, was interpreted as a phase of depressurization of the shallow magma reservoir, accompanied by a mechanical response of the edifice and an increase in surface eruptive activity. Note that there is a slight lag between the increase in tremor and the increase in flow rates, which may be due to uncertainties in lava flow rate measurements. Indeed, lava flow rate estimates derived from satellite methods may be underestimated due to observational biases, particularly those related to weather conditions (cloud cover), the development of flow within lava tubes, and the flow's entry into the sea, which limit the detection of thermal radiation.

The increase in lava flow rates was correlated with a rise in SO_2 fluxes measured by satellite (TROPOMI) and by the OVPF's NOVAC network (Figure 16).

As deflation slowed down until the eruption stopped on March 25, a gradual decrease in lava flow rates was observed, along with a decrease in summit seismicity (Figure 15). The period when the eruption stopped, from March 25 to 28, was marked by a resumption of edifice inflation and an increase in deep seismicity between 8 and 10 km below the western part of the summit (Figure 4). These observations suggest a new influx of deep magma into the shallow reservoir, leading to a re-pressurization of the magmatic system before the eruption restarted.

Upon the eruption resumed on March 28, flow rates were estimated at < 3 m³/sec, with a slight increase on March 30 (peak at 17 m³/sec, Figure 15). This resumption of the eruptive activity was marked by a new deflation of the edifice and a resumption of summit seismicity (Figure 15), in a dynamic comparable to that observed between March 18 and 25.

The cessation of surface activity on March 25, followed by its resumption on March 28, likely reflects an unstable magma supply regime. In other words, magma and gases continue to circulate, but the flow is not consistent enough to sustain surface emissions over the long term. In this case, the eruption may resume, weaken, and then stop again. This has already been observed at Piton de la Fournaise, notably during the August-October 2004 and August-October 2015 eruptions.

At the time of writing this monthly bulletin, the eruption ceased again during the night of April 2–3 around 12:10 a.m. local time (8:10 p.m. UTC on April 2). The end of this eruption will be discussed in the next monthly bulletin.

Volume and duration of the eruption

As of April 3, 2026, the volume of lava emitted at the surface, estimated based on surface lava flow rates (Figure 14), ranged between **22 and 28 million m³**, and the surface of the **platform**, estimated using stereophotogrammetry, **was approximately 8.5 hectares**.

The duration of this eruption—45,7 days of eruptive activity as of April 3 (compared to an average of 20 days for recent eruptions of Piton de la Fournaise)—can be explained by pressurization of the shallow magma reservoir between February 24 and March 15, detected by the inflation of the volcano during this period (Figure 15). **This pressurization is believed to be linked to the arrival of magma from deeper levels, thereby feeding the eruption.**

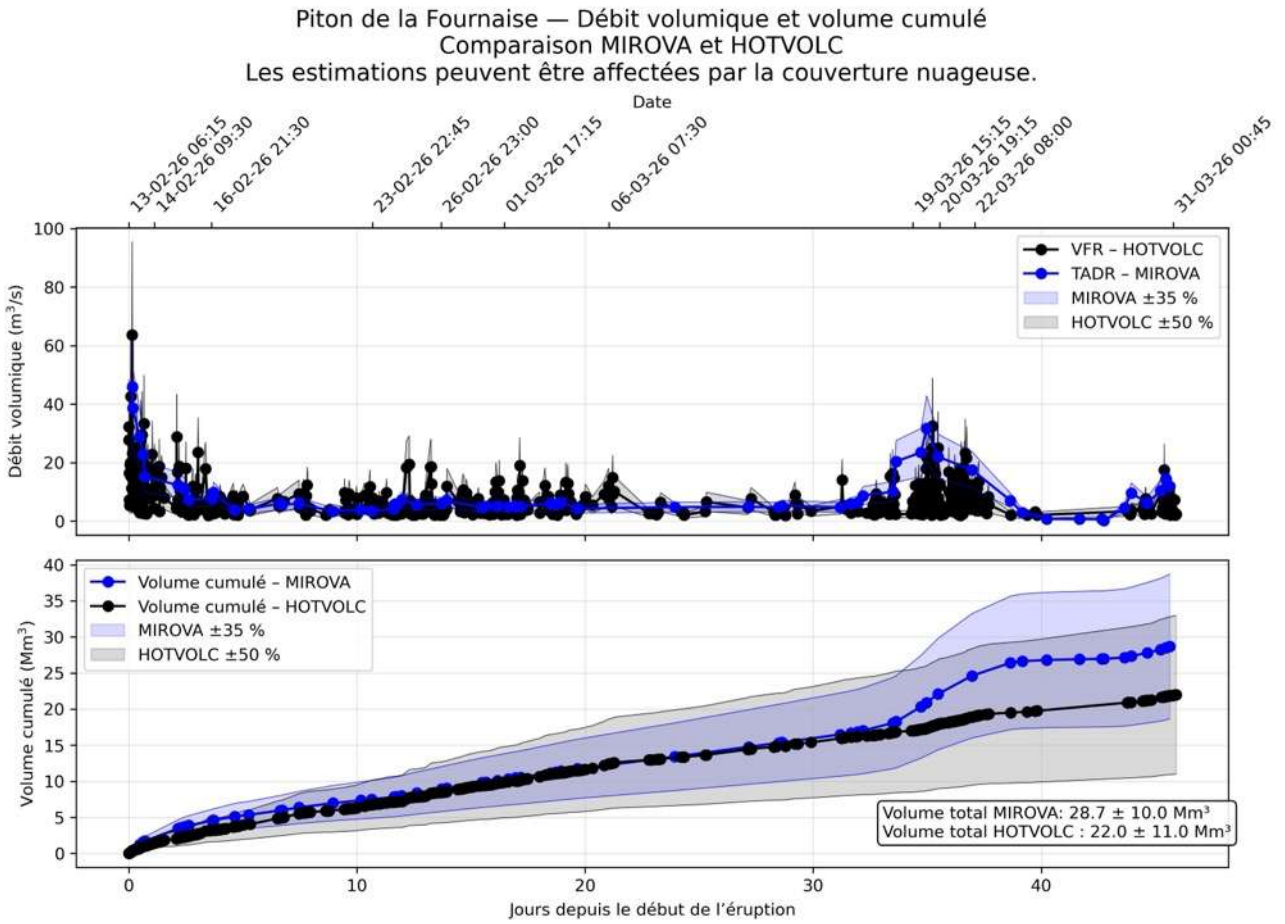

Figure 14: Estimates of surface lava flow rates (m³/s) and the cumulative volume of lava emitted at the surface (millions of m³, Mm³) based on satellite data from the HOTVOLC (in black, ©OPGC-Clermont Auvergne University) and MIROVA (in blue, ©University of Turin) plate-forms between February 13 and March 31, 2026.

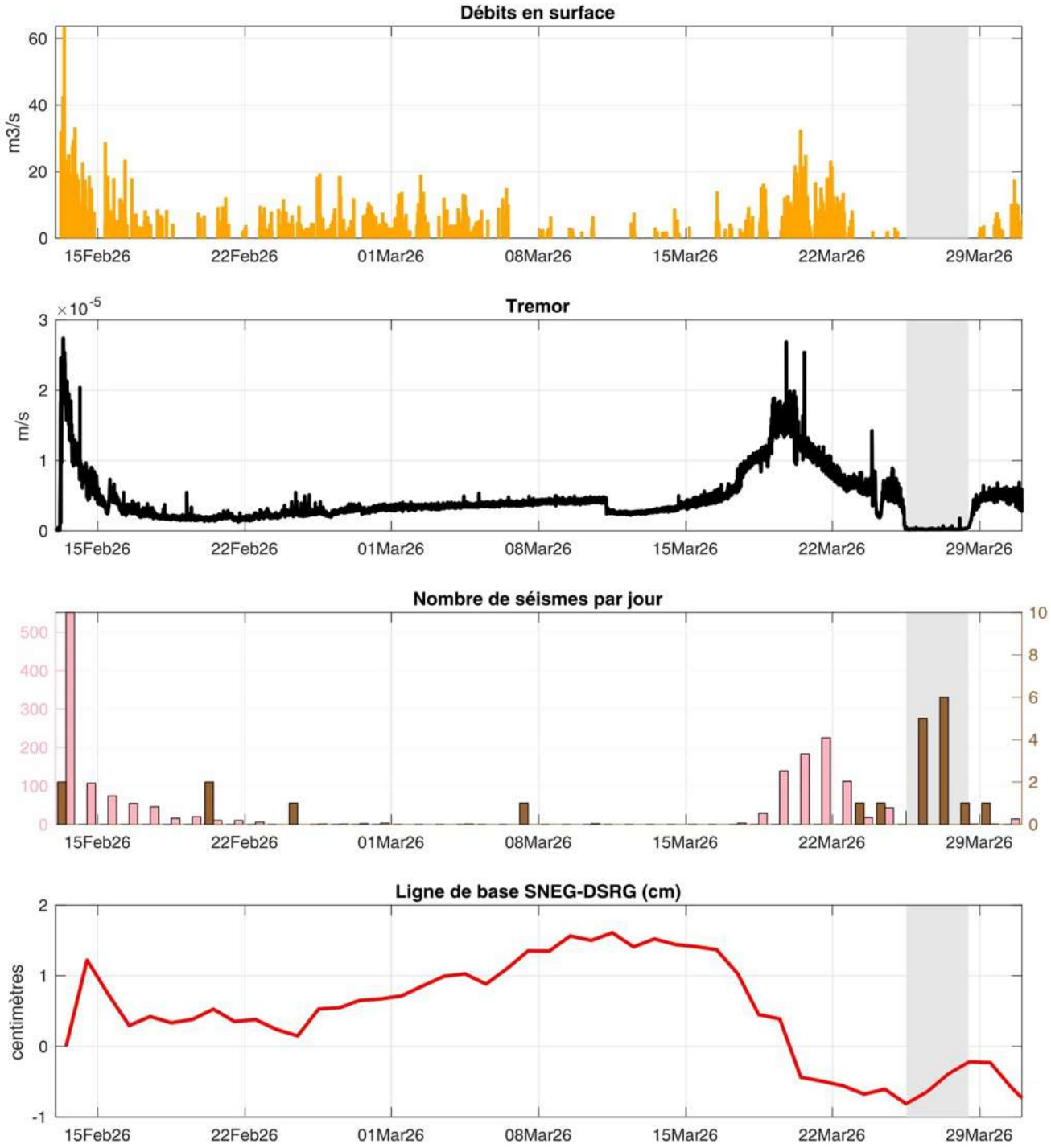

Figure 15: Comparison of surface lava flow rates estimated by Hotvolc (in m³/s, ©OPGC-Clermont Auvergne University), volcanic tremor intensity (in m/s, ©OVPF-IPGP), the number of shallow (in pink) and deep (in brown) volcano-tectonic earthquakes per day (©OVPF-IPGP), and the evolution of the SNEG-DSRG summit baseline (in cm) between February 13 and March 31, 2026. The pause in the eruption, observed between March 25 and 28, is shown in gray (©OVPF-IPGP).

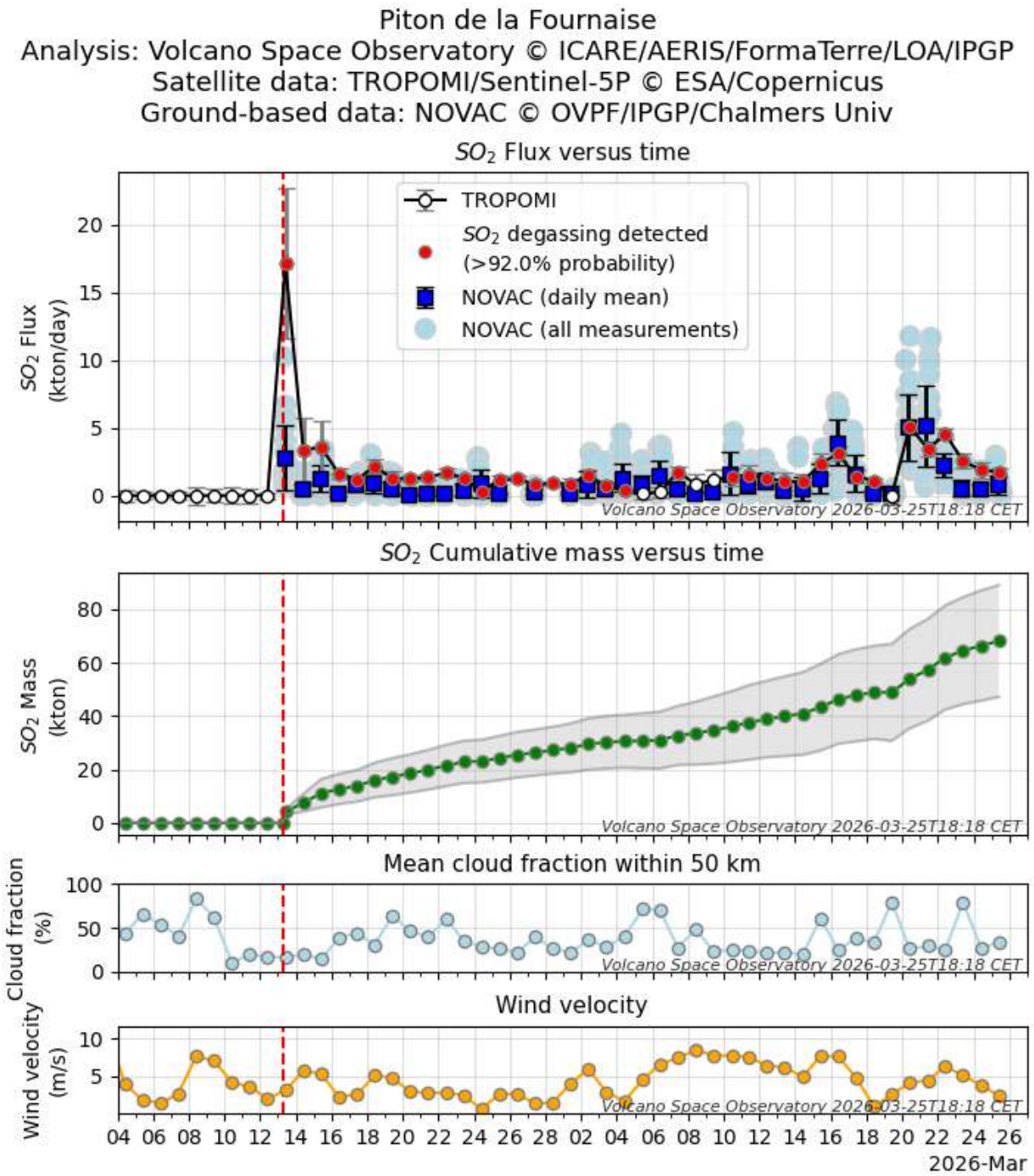

Figure 16: Trends in sulfur dioxide (SO_2) flux measured by satellite (TROPOMI) and estimated by the NOVAC DOAS network. Top: daily SO_2 flux. Center: cumulative mass of SO_2 emitted. Bottom: average cloud cover within a 50-km radius. The vertical red line indicates the start of the eruption on February 13, 2026, at Piton de la Fournaise. (© Volcano Space Observatory; ICARE/AERIS/FormaTerre/LOA/IPGP; TROPOMI/Sentinel-5P – ESA Copernicus; NOVAC – Chalmers University of Technology – OVPF-IPGP).

Numerical simulations of lava flows during the eruption

From the start of the eruption, lava flow paths were modeled using the DOWNFLOWGO model (LMV-Clermont Auvergne University) and were shared with authorities via *Etat Major de Zone et de Protection Civile de l'Océan Indien* (EMZPCOI) during crisis management. The map shows that the numerical simulations (Figure 17) generally accurately predicted the trajectories of the two main lava flows, although the models overestimated the likelihood of the northern flow developing. The model indicated that the lava flow associated with this branch could have reached the sea at a flow rate of at least 35 m³/s. However, the average flow rate during the first 24 hours is estimated to be between 14 m³/s (HOTVOLC) and 30 m³/s (MIROVA), before dropping to approximately 10 m³/s on the second day, causing this branch to stop.

These discrepancies between the simulations and observations can be attributed to the uncertainties inherent in the model, as well as to the inherently variable and difficult-to-predict dynamics of eruptions.

Simulations performed using DOWNFLOWGO (Figure 17) allow for the probabilistic quantification of potential lava flow paths starting from a given source point.
The model calculates both the spatial distribution of preferred flow paths based on topography and the maximum distance the lava could reach along the main trajectory, based on its cooling rate and a given flow rate (blue arrows and associated value in m³/s on the map in Figure 17).
The model's results must, however, be interpreted with an awareness of its limitations: the spatial accuracy of the runout distance remains constrained by an uncertainty of approximately 30% (represented by the light blue line on the map in Figure 17). Consequently, these simulations are relevant for short-duration eruptions, in which the lava flows as a single main flow.

In the case of prolonged eruptions, such as the one that began on February 13, 2026, processes not explicitly accounted for by the model can significantly alter the dynamics of the lava flow. In particular, the gradual solidification of certain branches can create obstacles, forcing subsequent lava flows to redirect toward new areas. These reorganizations of the flow network introduce alternative trajectories that are not necessarily predicted by the initial simulation.
The formation of lava tubes leads to resurgences on the surface downstream of the main vent. These resurgence points then constitute new effective sources of supply. It is therefore possible to restart simulations from these resurgence points to re-evaluate potential trajectories and associated propagation distances (Figure 18).

These new maps were recalculated and shared with the authorities as field observations were made and the lava flow evolved.

With the aim of improving these flow models, measurements of viscosity, temperature, and velocity of the lava flows were taken during this eruption (Figure 19).

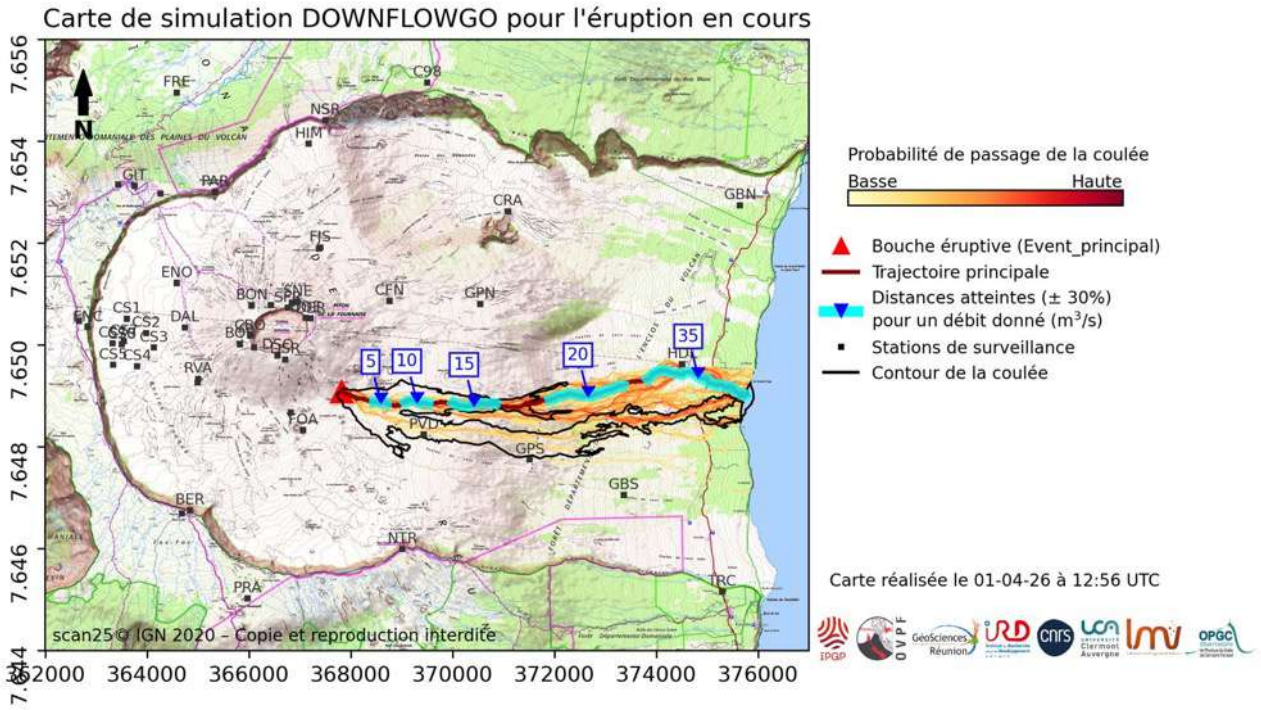

Figure 17: Numerical simulations of probable lava flow inundation paths for the Februay 13, 2026 eruption (following the protocol described in Harris et al. 2019). The inundation area is computed for 10000 iterations from the initial vent location with vertical elevation noise of 2 m via the DOWNFLOW model (Favalli et al. 2005). Yellow to red lines represent the frequency of lava paths from low (yellow) to high (red). The line of steepest descent (LoSD) is shown in red. Blue arrows represent the location at which the lava could extend along the LoSD for given effusion rates (numbers are in m^3/s) as computed using the FLOWGO model (Harris and Rowland 2001; Chevrel et al. 2018). The light blue lines represent a 30% uncertainty in the distance. The black outline shows the contour of the lava flow as of March 23, 2026 (©OPGC-LMV-OVPF-IPGP).

Références:

. Chevrel MO, Labroquere J, Harris AJL, Rowland SK (2018) PyFLOWGO: An Open-Source Platform for Simulation of Channelized Lava Thermo-RheologicalProperties. Comput. Geosci. 111: 167–80. https://doi.org/10.1016/j.cageo.2017.11.009

. Favalli M, Pareschi MT, Neri A, Isola I (2005) Forecasting Lava Flow Paths by a Stochastic Approach. Geophys. Res. Lett. 32(3): 1–4.https://doi.org/10.1029/2004GL021718

. Harris AJL, Chevrel MO, Coppola D, Ramsey MS, Hrysiewicz A, Thivet S, Villeneuve N et al. (2019) Validation of an Integrated Satellite-data-driven Response to an Effusive Crisis: The April–May 2018 Eruption of Piton de La Fournaise. Ann. Geophys. 61. https://doi.org/10.4401/ag-7972

. Harris AJL, Rowland SK (2001) FLOWGO: A Kinematic Thermo-Rheological Model for Lava Flowing in a Channel. Bull. Volcanol. 63: 20–44.https://doi.org/10.1007/s004450000120

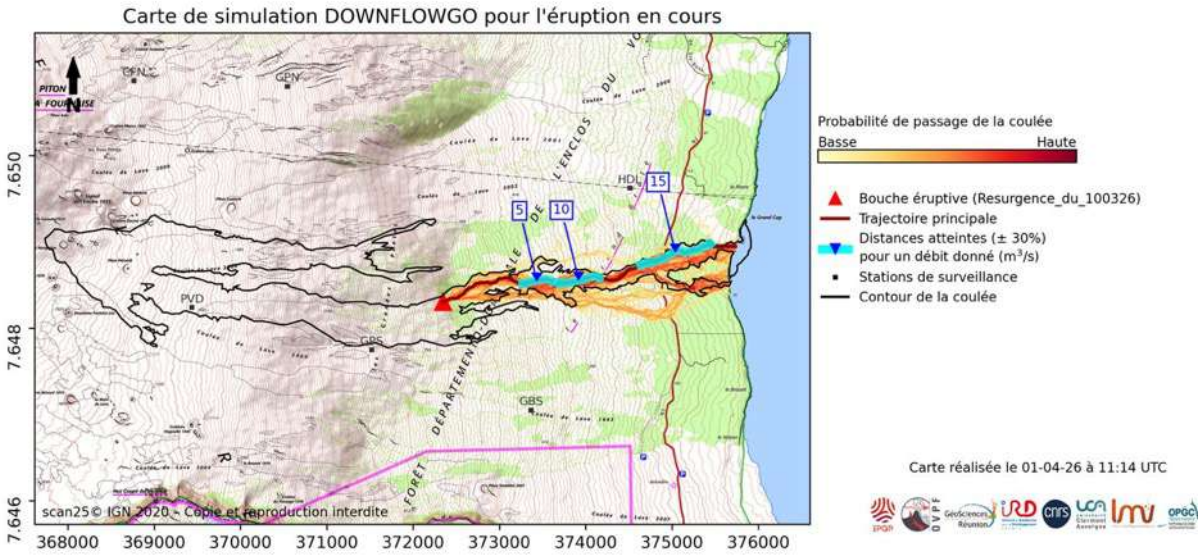

Figure 18: Numerical simulations of probable lava flow inundation paths based on the main resurgence point as of March 10, 2026, on the main southern branch. See the legend in Figure 17 for further details (©OPGC-LMV-OVPF-IPGP).

Figure 19: Viscosity and temperature measurements in the field on March 16, 2026 (@OVPF-IPGP, Cité du Volcan, LMV-UCA-IRD).

Institut de physique du globe
de Paris, OVPF
14 RN3 – Km 27
97418 La Plaine des Cafres
La Réunion

www.ipgp.fr/ovpf
facebook : ObsVolcanoPitonFournaise
bluesky : @ovpf.bsky.social
youtube : Chaîne IPGP

C. Seismic activity on La Réunion and in the Indian Ocean basin

Local and regional seismicity

In March 2026, the OVPF-IPGP recorded:

- 21 local earthquakes (below the island, within a radius of 200 km around the island, Figures 20 and 21);
- 4 regional earthquakes (in the Indian Ocean basin).

In **March 2026**, the OVPF-IPGP detected **21 local earthquakes.** Four events were located: one beneath *La Roche Écrite*, one off the coast of *Saint Denis*, one beneath the *Grand Étang* region, and the last one at a depth of approximately 15 km beneath the eastern flank of Piton de la Fournaise (Figure 21). Most of these earthquakes have **magnitude less than 1** and are difficult to locate accurately. These earthquakes were located between **10 km and 25 km depth in oceanic lithosphere** on which was built the volcanic edifice at the origin of La Réunion island.

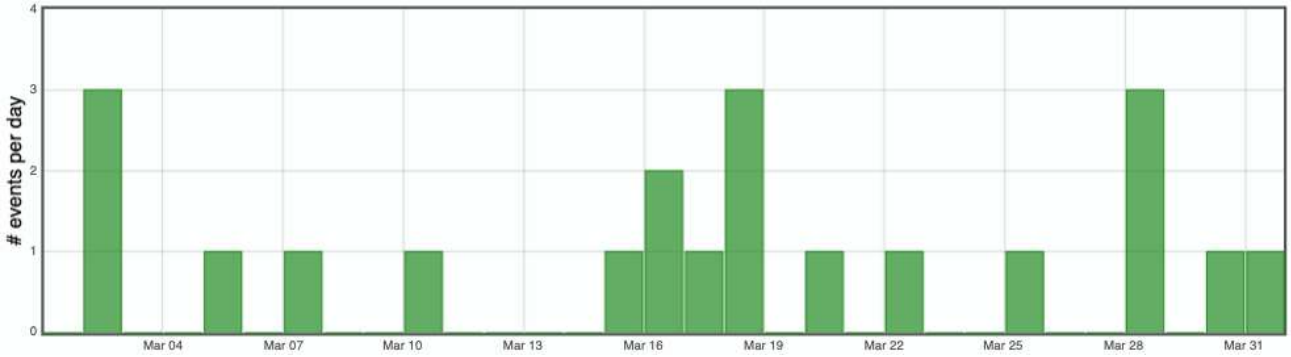

Figure 20: Number of local earthquakes (La Réunion island) per day recorded in March 2026 (©WebObs/OVPF-IPGP).

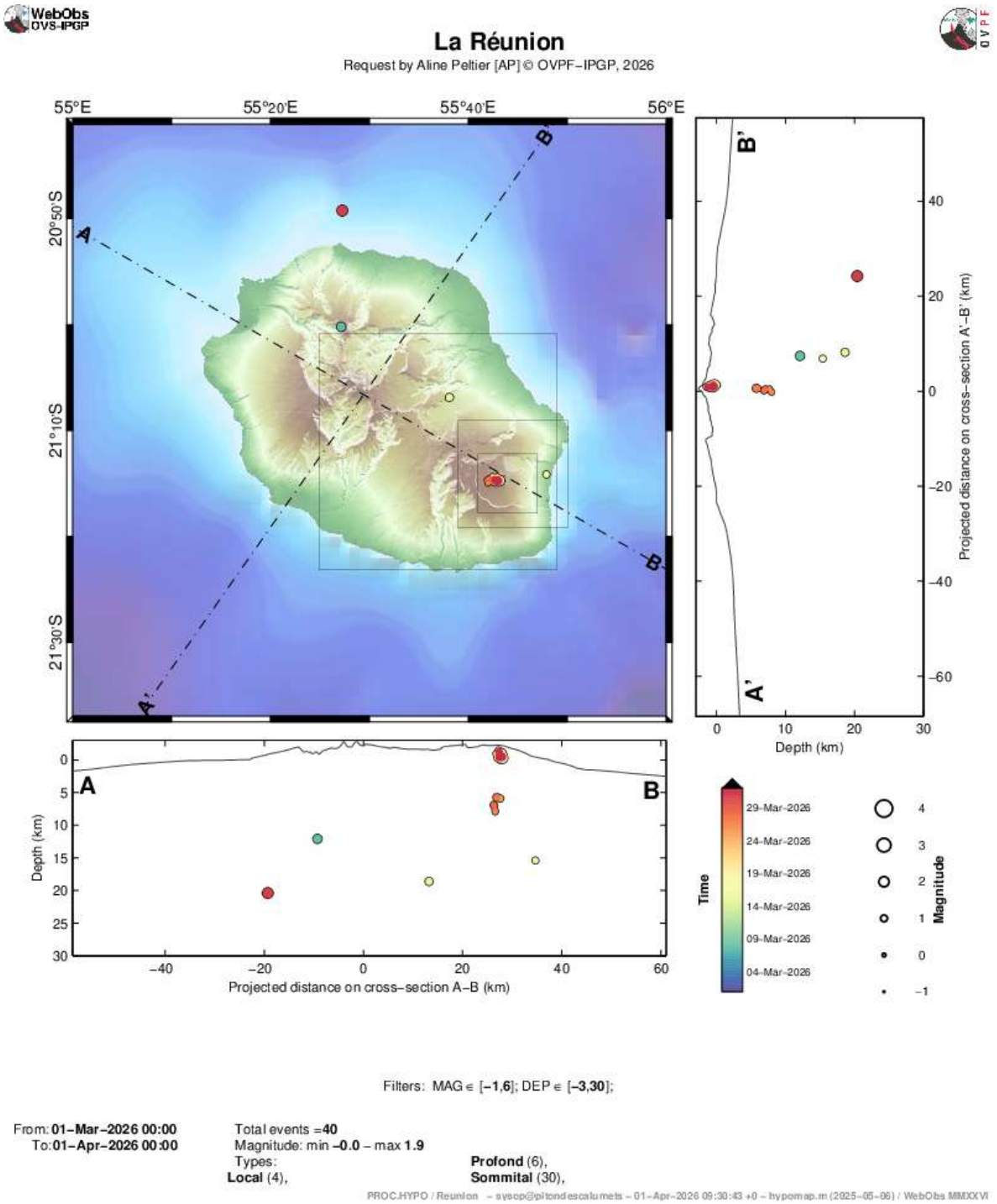

Figure 21: Seismicity below La Réunion in March 2026. Location map (epicenters) and north-west – south-east and south-west – north-east cross-sections (hypocenters) of earthquakes as recorded by OVPF-IPGP. Only localizable earthquakes are shown on the map (©WebObs/OVPF-IPGP).

Seismic-volcano activity in Mayotte

The « REseau de surveillance VOlcanologique et SIsfmologique de MAyotte (REVOSIMA) » is the structure in charge of the volcano and seismic monitoring of Mayotte. IPGP and BRGM coordinate and manage REVOSIMA. Operational monitoring of seismo-volcanic activity is carried out by IPGP (OVPF), under the joint responsibility of BRGM and in close association with IFREMER and CNRS. REVOSIMA is supported by a scientific and technical partnership. The REVOSIMA consortium: IPGP and Université Paris Cité, BRGM, IFREMER, CNRS, BCSF-RéNaSS, ITES and Université de Strasbourg, IGN, ENS, SHOM, TAAF, CNES, Université Grenoble Alpes and ISTerre, Université Clermont Auvergne, LMV and OPGC, Université de La Réunion, Université Paul Sabatier, Toulouse and GET-OMP, Université de la Rochelle, Université de Bretagne Occidentale, IRD and collaborators.

All information on the REVOSIMA and the activity in Mayotte can be found on the dedicated webpages:
- https://www.ipgp.fr/observation/infrastructures-nationales-hebergees/revosima/
- https://www.ipgp.fr/actualites-du-revosima/
- https://www.facebook.com/ReseauVolcanoSismoMayotte/
- https://bsky.app/profile/revosima.bsky.social

April 8, 2026
OVPF-IPGP Director

D. Appendix

Definition of Volcanic Alert Levels for Piton de la Fournaise

from *disposition spécifique « Volcan Piton de la Fournaise » - arrêté n°2242-* Emergency plan set up by the department responsible for the protection of the population in the event of unrest or activity of the Piton de la Fournaise

•**"Vigilance"**: possible eruption in medium term (a few days or weeks) **or** presence of risks on the sector (rockfalls, increase of gas emissions, still hot lava flows…).

Access to the Enclos Fouqué caldera and to the summit volcano are allowed with restrictions.

• **"Alert 1"**: probable or imminent eruption.

Access to the Enclos Fouqué caldera and to the summit are closed and prohibited.

• **"Alert 2"**: ongoing eruption.
Alert 2-1: ongoing eruption inside the Enclos Fouqué caldera without threat to the safety of people, property or the environment

Alert 2-2: ongoing eruption inside the Enclos Fouqué caldera with direct or indirect threat to the safety of people, property or the environment.

Access to the Enclos Fouqué caldera and to the summit are closed and prohibited. For Alert 2-2, evacuation of the people and vehicles depending on the issues.

• **"Alert 2-3"**: ongoing eruption outside the Enclos Fouqué caldera with threat to the safety of people, property or the environment.

Access to the Enclos Fouqué caldera and to the summit are closed and prohibited. Evacuation of the people and vehicles depending on the issues.

• **"Sauvegarde"**: end of eruption.

Evaluation of a partial reopening of the Enclos Fouqué caldera access.

References

Altamimi, Z., Rebischung, P., Collilieux, X., Métivier, L., & Chanard, K. (2023), ITRF2020: an augmented reference frame refining the modeling of nonlinear station motions, Journal of Geodesy, 97(5), 47. https://link.springer.com/article/10.1007/s00190-023-01738-w

Arellano, S., Galle, B., Apaza, F., Avard, G., Barrington, C., Bobrowski, N., ... Yalire, M. (2020), Synoptic analysis of a decade of daily measurements of SO_2 emission in the troposphere from volcanoes of the global ground-based Network for Observation of Volcanic and Atmospheric Change, Earth System Science Data Discussions, 2020, 1-3

Beauducel, F., Roult, G., Ferrazzini, V., Peltier, A., Jousset, P., Boissier, P., Villeneuve, N. (2025), Jerk, a promising tool for early warning of volcanic eruptions. Nat Commun 16, 11418, https://doi.org/10.1038/s41467-025-66256-z

Bénard, B., Di Muro, A., Liuzzo, M., Gurrieri, S., Boissier, P., Brunet, C. et al. (2023), Seasonal environmental controls on soil CO_2 dynamics at a high CO_2 flux sites (Piton de la Fournaise and Mayotte volcanoes), Journal of Geophysical Research: Biogeosciences, 128(6), e2023JG007409

Bertiger, W., Bar-Sever, Y., Dorsey, A., Haines, B., Harvey, N., Hemberger, D., ... & Willis, P. (2020), GipsyX/RTGx, a new tool set for space geodetic operations and research, Advances in space research, 66(3), 469-489

Boudoire, G. (2017), Architecture et dynamique des systèmes magmatiques associés aux volcans basaltiques : exemple du Piton de la Fournaise. Volcanologie, Université de la Réunion, 2017. Français. ⟨NNT : 2017LARE0022⟩. ⟨tel-01902958⟩

Chevrel, MO., Labroquere, J., Harris, AJL, Rowland, SK (2018), PyFLOWGO: An Open-Source Platform for Simulation of Channelized Lava Thermo-RheologicalProperties. Comput. Geosci. 111: 167–80. https://doi.org/10.1016/j.cageo.2017.11.009

Duputel, Z., Lengliné, O., Ferrazzini, V. (2019), Constraining Spatiotemporal Characteristics of Magma Migration at Piton De La Fournaise Volcano From Pre-eruptive Seismicity, Geophys. Res. Lett. 46: 119-127, https://doi.org/10.1029/2018GL080895

Favalli, M., Pareschi, MT., Neri, A., Isola, I. (2005), Forecasting Lava Flow Paths by a Stochastic Approach, Geophys. Res. Lett, 32(3): 1–4.https://doi.org/10.1029/2004GL021718

Harris, AJL., Chevrel, MO., Coppola, D., Ramsey, MS., Hrysiewicz, A., Thivet, S., Villeneuve, N. et al. (2019), Validation of an Integrated Satellite-data-driven Response to an Effusive Crisis: The April–May 2018 Eruption of Piton de La Fournaise, Ann. Geophys. 61, https://doi.org/10.4401/ag-7972

Harris, AJL., Rowland, SK. (2001), FLOWGO: A Kinematic Thermo-Rheological Model for Lava Flowing in a Channel. Bull. Volcanol. 63: 20–44.https://doi.org/10.1007/s004450000120

Lomax, A., Virieux, J., Volant, P., & Berge-Thierry, C. (2000), Probabilistic earthquake location in 3D and layered models. In C. H. Thurber & N. Rabinowitz (Eds.), Advances in Seismic Event Location, Modern Approaches in Geophysics (pp. 101–134). Springer, Dordrecht, Netherlands

Murphy, D., Bertiger, W., Hemberger, D., Komanduru, A., Peidou, A., Ries, P., & Sibthorpe, A. (2024), Jet Propulsion Laboratory Analysis Center Technical Report 2024. In R. Dach & E. Bockmann (Eds.), International GNSS Service Technical Report 2024 (IGS Annual Report), IGS Central Bureau and University of Bern; Bern Open Publishing. https://doi.org/10.48350/191991

Rebischung, P., Altamimi, Z., Métivier, L. et al. (2024), Analysis of the IGS contribution to ITRF2020, J Geod 98, 49. https://doi.org/10.1007/s00190-024-01870-1

SeisComP (2024), SeisComP 6 – Earthquake Monitoring Software, https://www.seiscomp

Acknowledgments
Thank you to organizations, communities and associations for publicly posting this report for the widest dissemination

Information
All information on the Piton de la Fournaise activity can be found on the OVPF-IPGP media:
- Internet website : ipgp.fr/fr/ovpf/actualites-ovpf
- Bluesky : @ovpf.bsky.social
- Facebook : facebook.com/ObsVolcanoPitonFournaise

A preliminary automatic daily bulletin of the OVPF-IPGP, relating to the activities of the day before, validated by an analyst, is published daily. It can be accessed directly at this link:
http://volcano.ipgp.fr/reunion/Bulletin_quotidien/bulletin.html

The seismicity validated in continuous by OVPF-IPGP can also be followed on the RENASS portal: https://renass.unistra.fr/fr/zones/la-reunion

The OVPF-IPGP data are distributed by the IPGP data centre - Volobsis - and are also available on the EPOS and Epos-France websites (doi:10.18715/REUNION.OVPF).